

Experimental Physiology

Transformation of adult rat cardiac myocytes in primary culture

Tamas Banyasz¹, Ilya Lozinskiy², Charles E. Payne², Stephanie Edelmann², Byron Norton², Biyi Chen², Ye Chen-Izu², Leighton T. Izu² and C. William Balke²

¹Department of Physiology, University of Debrecen, Debrecen, Hungary

²Department of Internal Medicine, University of Kentucky, Lexington, KY 40536, USA

We characterized the morphological, electrical and mechanical alterations of cardiomyocytes in long-term cell culture. Morphometric parameters, sarcomere length, T-tubule density, cell capacitance, L-type calcium current ($I_{Ca,L}$), inward rectifier potassium current (I_{K1}), cytosolic calcium transients, action potential and contractile parameters of adult rat ventricular myocytes were determined on each day of 5 days in culture. We also analysed the health of the myocytes using an apoptotic/necrotic viability assay. The data show that myocytes undergo profound morphological and functional changes during culture. We observed a progressive reduction in the cell area (from $2502 \pm 70 \mu\text{m}^2$ on day 0 to $1432 \pm 50 \mu\text{m}^2$ on day 5), T-tubule density, systolic shortening (from 0.11 ± 0.02 to $0.05 \pm 0.01 \mu\text{m}$) and amplitude of calcium transients (from 1.54 ± 0.19 to 0.67 ± 0.19) over 5 days of culture. The negative force–frequency relationship, characteristic of rat myocardium, was maintained during the first 2 days but diminished thereafter. Cell capacitance (from 156 ± 8 to $105 \pm 11 \text{ pF}$) and membrane currents were also reduced ($I_{Ca,L}$, from 3.98 ± 0.39 to $2.12 \pm 0.37 \text{ pA pF}^{-1}$; and I_{K1} , from 34.34 ± 2.31 to $18.00 \pm 5.97 \text{ pA pF}^{-1}$). We observed progressive depolarization of the resting membrane potential during culture (from 77.3 ± 2.5 to $34.2 \pm 5.9 \text{ mV}$) and, consequently, action potential morphology was profoundly altered as well. The results of the viability assays indicate that these alterations could not be attributed to either apoptosis or necrosis but are rather an adaptation to the culture conditions over time.

(Received 11 September 2007; accepted after revision 6 December 2007; first published online 21 December 2007)

Corresponding author T. Banyasz: University of Kentucky, BBSRB-Room B251, 741 South Limestone Street, Lexington, KY 40536-0509, USA. Email: tbany2@email.uky.edu

Cultured adult cardiac myocytes currently are a model routinely used in cardiovascular research. The increasing popularity of this model is clearly demonstrated with numerous publications within the first half of last year (Arruda *et al.* 2007; Chilton *et al.* 2007; Cuello *et al.* 2007a,b; Eder *et al.* 2007; Heidkamp *et al.* 2007; Herron *et al.* 2007; Huang *et al.* 2007; Oestreich *et al.* 2007; Tastan *et al.* 2007; Vila-Petroff *et al.* 2007; Warrier *et al.* 2007; Yang *et al.* 2007; Zhu *et al.* 2007). Apart from other important aspects (i.e. efficiency, practical or ethical considerations), the major advantage of using cultured cells is the long viability. While freshly isolated cardiac myocytes remain in ‘good condition’ for only 10–12 h, cultured myocytes can be used for longer term studies which may involve manipulation of humoral influences, gene transfer or protein expression (Bölck *et al.* 2004; Weisser-Thomas

et al. 2005; Arruda *et al.* 2007). However, the reliability of data obtained in cultured cells is highly dependent on preservation of the original phenotype. While long-term viability is an advantage, the long culture time allows cells to adapt to culture conditions; therefore, phenotype can alter. An increasing body of data suggests that isolated cardiac myocytes undergo profound morphological and functional transformation during long-term culture and therefore cannot be considered to be in a steady state (Ellingsen *et al.* 1993; Horackova *et al.* 1996; Horackova & Byczko, 1997; Mitchelson *et al.* 1998; Poindexter *et al.* 2001; Schiess *et al.* 2005). As a standard method, experiments using cultured cells often make comparison between cells exposed to test conditions and those kept under control culture conditions during the same period. However, if the cultured cells used as controls undergo transformation

during long-term culture, the concomitant changes in the control cells need to be taken into account in interpretation of the data.

Great efforts have been made by several groups to maintain the morphology and function of cardiac myocytes in primary culture. Among many other attempts, co-culture with cardiac neurones (Horackova *et al.* 1997), continuous electrical field stimulation (Berger *et al.* 1994; Horackova *et al.* 1996), β -adrenergic stimulation with isoprenaline (Akuzawa-Tateyama *et al.* 2006), culture in high- Ca^{2+} medium (Davidoff *et al.* 1997) or application of biocompatible materials (Polonchuk *et al.* 2000) have been used to maintain phenotype. Some of these methods seem to help by slowing down cell degeneration, but the cultured adult myocyte model is still not stable and cannot be used to substitute freshly isolated cells.

Under these circumstances, it is important to understand the mechanism and time line of the transformation of cardiac myocytes in long-term culture. Furthermore, we have to identify individual window periods for each experimental method to establish a time frame when cultured cells can be used as an appropriate model.

The goal of this study was twofold. First, we wanted to systematically characterize the functional changes of adult rat ventricular myocytes (ARVM) in long-term culture. Earlier studies on this topic had only limited scope, focusing on morphological, mechanical or electrical properties of cultured cells. Since different laboratories use different culturing methods, it is very difficult (if not impossible) to relate morphological observations to functional data when they originate from different laboratories. Here, we report our data from a comprehensive study in which morphometry, sarcomere length, T-tubule density, contractility and electrophysiology were systematically studied on each culture day. These data can provide guidelines for those who use ARVM as an experimental model.

Second, using the culture method developed in our laboratory, we tested the hypothesis that the functional changes observed in ARVM during long-term culture are not attributable to apoptosis or necrosis. Thus, we aimed to understand the mechanism of cell death in our cultured cardiac myocytes.

Our observations show that when ARVM die in culture, the first step is a loss of ability to maintain a normal diastolic calcium level. Morphologically, the cells first shorten and then round up. Apoptosis or necrosis was not detected in rod-shaped cells, and only showed up after cells became rounded up. The T-tubule structure and force–frequency relationship are preserved for 2 days in culture. Electrophysiological properties undergo progressive adaptation during the first 3 days of culture and then reach a steady state during the fourth and fifth day in culture.

Methods

All animals and procedures were handled strictly in accordance with the National Institutes of Health (NIH) guidelines and protocols were approved by the University of Kentucky's Institutional Animal Care and Use Committee. Chemicals and reagents were purchased from Sigma-Aldrich if not specified otherwise.

Cell preparation and culture techniques

Sprague–Dawley rats were purchased from Harlan (Indianapolis, IN, USA). Rats were anaesthetized using a Surgivet Isotech 4 vaporizer unit delivering 6% isoflurane in medical grade oxygen. After suppression of the spinal cord reflexes, the hearts were removed via mid-line thoracotomy. A standard enzymatic technique described in detail previously (Lopez-Lopez, 1995) was used to isolate ventricular myocytes.

Following isolation, cells were allowed to settle for 1 h. Cells were suspended in serum-free Medium 199 (Gibco 12350, Invitrogen) containing (mm): taurine, 5; creatine, 5; L-carnitine, 5 (Volz *et al.* 1991; Ellingsen *et al.* 1993); and sodium bicarbonate, 26; and plated in 26-well plates onto 12 mm glass coverslips that had been coated with 20 $\mu\text{g ml}^{-1}$ mouse laminin (Mitchelson *et al.* 1998). Cultures were incubated at 37°C, in an atmosphere of 5% CO_2 –95% air for 2 h. Fresh medium was added gently as medium was being drawn off until the cultures had been thoroughly washed. The cells were then cultured under the same culture conditions, and assessed every 24 h, for 5 days. Only quiescent, rod-shape myocytes were selected for experiments.

Morphometry

Randomly selected areas of cell culture were visualized using a $\times 40$ objective on a Nikon Diaphot microscope and photographs were taken using a Nikon Coolpix 8800 with a MM99 microscope adapter. Cell length, width and area were determined using ImageJ software (NIH). The mean sarcomere length was determined from the largest Fourier coefficient of the fast Fourier transform average of the intensity value derived from ImageJ.

Apoptosis

Cardiomyocytes were assayed using the Vybrant apoptosis assay kit no. 7 (Invitrogen, no. V-23201) to determine whether the isolation or culturing procedures were inducing apoptosis. Medium 199 containing no phenol red (Invitrogen, no. 11043) replaced phosphate-buffered saline. Cells were plated and stained on laminin-coated coverslips. The YO-PRO-1 concentration was doubled in fresh cultures, and cells were incubated with the dyes at room temperature. To verify YO-PRO-1 assay, control cells were induced with 5 μM doxorubicin (Fluka,

no. 44583) for 14 h at 37°C, in 5% CO₂–95% air (Kumar *et al.* 1999; Lou *et al.* 2006). Images were recorded with Spot version 4.1 on a Nikon Eclipse E600 microscope (Diagnostic Instruments, Sterling Heights, MI, USA). Images were postprocessed using MetaMorph version 6.3 (Universal Imaging Corporation, West Chester, PA, USA).

Contraction measurements

Myocytes were loaded with 2.5 μ M fluo-5FAM fluorescent calcium-sensitive dye for 45 min at room temperature. Then cells were transferred to a chamber mounted on the stage of an inverted microscope (Olympus IX71) and superfused with Tyrode solution (mm: NaCl, 145; KCl, 4; CaCl₂, 1; NaH₂PO₄, 0.33; MgCl₂, 1; Hepes, 10; and dextrose, 10; at pH 7.2) at room temperature. The cells were field stimulated with 4 ms bipolar, supramaximal pulses using a Grass S48 stimulator. Prior to recording, the cells were stimulated for 10 min at a constant pacing rate in order to allow them to adapt to the new frequency and reach a steady state. Calcium transients and sarcomere shortening were recorded simultaneously in the same cell using an IonOptix system (IonOptix, Milton, MA, USA). All fluorescence measurements were carried out with the same excitation light intensity and gain level. Recordings were analysed using the IonOptix analysis package.

Staining of T-tubules and analysis

For each time point beginning with freshly isolated cells (D0) and continuing to day 5 in culture (D5), cells were incubated with di-8-ANEPPS (Invitrogen no. D3167) at a working concentration of 10 μ M for 20 min. The di-8-ANEPPS was washed out with Tyrode solution, and images were obtained with a Zeiss LSM 5 Live using a $\times 100$ NA 1.4 oil plan-apo objective. Several focal planes were recorded in each cell, and we used only those frames where the nucleus was not seen. The images were then analysed with ImageJ image analysis software (NIH), measuring the area fraction within the cell that had taken up the dye. The data for each time point were then statistically compared to determine changes in T-tubule fractional area.

Detubulation

Cells were incubated in Tyrode solution containing formamide (1.5 M) for 20 min at room temperature, and then washed in fresh Tyrode solution. The formamide treatment caused detubulation of the ventricular myocytes as previously reported (Kawai *et al.* 1999).

Electrophysiology

All experiments were performed in whole cell configuration at room temperature. An Axoclamp 200B amplifier and Digidata 1324 A/D–D/A converter

were used with pClamp 9.2 software package for data acquisition and analysis (Molecular Devices). Electrodes were prepared from borosilicate glass, having a tip resistance of 1.5–2.5 M Ω when filled with pipette solution (containing, mm: potassium aspartate, 108; KCl, 45; NaCl, 10; EGTA, 2; Mg-ATP, 3; and Hepes, 5 for action potential and I_{K1} recordings or CsCl, 135; TEACl, 10; EGTA, 2; Mg-ATP, 5; and Hepes, 10 for measurement of L-type calcium current ($I_{Ca,L}$), at pH 7.2) Action potentials and I_{K1} were recorded in Tyrode solution, whereas $I_{Ca,L}$ was measured in sodium-free medium (containing, mm: N-methyl-D-glucamine, 155; CaCl₂, 1; MgCl₂, 1; Hepes, 10; dextrose, 10; and 4 aminopyridine, 3; at pH 7.2). Calcium currents were recorded with a 500 ms long depolarization step to +10 mV preceded by a set of prepulses clamped to various voltages between -70 and +60 mV for 1000 ms. The value of I_{K1} was recorded with a 200 ms long hyperpolarizing step to -130 mV from a holding potential of -70 mV, and 50 μ M BaCl₂ was used for pharmacological dissection. Ionic currents were normalized to cell capacitance (measured in whole cell configuration by applying 10 mV voltage steps from a holding potential of 0 mV) during analysis. Action potentials were recorded in current clamp mode when cells were stimulated via the recording electrode using a GRASS S48 stimulator (Grass Technologies Product Group, Astro-Medical, Inc., Mentor, OH, USA). A 5 min adaptation period with a constant stimulation rate was applied before each action potential measurement between 0.5 and 2.0 Hz to stabilize parameters before recording. Before 0.1 Hz measurements, we applied a 10 min adaptation period. Data were corrected for a liquid junction potential of -10 mV.

Statistical analysis

All values presented are arithmetic means \pm s.e.m. Statistical significances were calculated by ANOVA and Student's paired or unpaired *t* test as appropriate. The difference in mean values was considered significant when the *P* value was less than 0.05.

Results

Morphometry

Cultured cells maintained rod shape but after the second day their ends became rounded and the regular striation started to fragment (Fig. 1). A minor fraction of cells (less than 5% of the total) underwent severe morphological transformation after the third day, extending fingerlike pseudopodia or forming dumbbell-like structures (see arrow in Fig. 1A). These pleomorphic cell types were not included in the analysis. Cell size (length, diameter and area) and sarcomere length were determined within 2 h after cell isolation. On days 1–5 the cell

measurements were performed at the same time of day as the original isolation (± 1 h). The average cell length decreased from 107.8 ± 2.2 to $93.1 \pm 1.75 \mu\text{m}$ ($P < 0.001$) during the first day of culture. Further shortening was observed up to the fifth culture day ($86.9 \pm 2.73 \mu\text{m}$ on day 5). The average diameter of cells decreased from 23.75 ± 0.59 to $16.57 \pm 0.47 \mu\text{m}$ ($P < 0.001$) during 5 days of culture. The average diastolic sarcomere length was shortened on the second and the third day of culture compared with those measured on the day of isolation (D0, $1.782 \pm 0.008 \mu\text{m}$; D1, $1.73 \pm 0.010 \mu\text{m}$; and D2, $1.74 \pm 0.024 \mu\text{m}$; $P < 0.05$). Following the second day of culture, the average sarcomere length showed no significant difference from that measured on day 0. Average cell area decreased gradually from 2502 ± 70 (D0) to $1432 \pm 50 \mu\text{m}^2$ (D5) during the period from D0 to D5 ($P < 0.001$). In an attempt to answer the question of whether the shift in these parameters resulted from a shorter survival rate of the larger myocytes or from a reduction in cell size generally, we conducted a follow-up study to record morphometric changes of individual cells, using culture dishes with a grid (Nunclon, Nalge Nunc International, Rochester, NY, USA), which are designed to localize the same cells during repetitive measurements in culture. Surprisingly, in spite of using laminine a considerable fraction of cells moved during the daily changes of culture medium, making it impossible to accomplish our goal. Thus, the mechanism of the shift in morphometric parameters in the population remains unresolved.

Viability tests

Cardiomyocytes were assayed to determine whether the isolation and culture methods were inducing apoptosis or whether the cells were undergoing normal cellular

necrosis. The Vybrant apoptosis assay kit no. 7 (Invitrogen) was used on freshly isolated (Fig. 2A–C) and 5 day cultures (Fig. 2G–I). Using the blue nuclear stain Hoechst 33342 both cell populations showed specific staining of the nucleus with low cytoplasmic fluorescence (Fig. 2A and G). Intact rod-shaped myocytes were propidium iodide negative, as evidenced by a lack of red nuclear staining. Likewise, cell populations from freshly isolated and day 5 cultures which were somewhat deteriorated (arrow in Fig. 2A) did not fluoresce with the propidium iodide dye because they had intact plasma membranes (Figs 2B and H). The fluorescent dye YO-PRO-1, which fluoresces when cells undergo apoptosis but also enters cells with damaged membranes, as evidenced by a uniform green fluorescence, was also negative in both the rod-shaped and partly deteriorated myocytes (Fig. 2C and I). To validate the effectiveness of the YO-PRO-1 dye, myocytes were induced with the pro-apoptotic chemical doxorubicin. The morphology of the rod-shaped cells was maintained after 14 h induction using $5 \mu\text{M}$ doxorubicin (Fig. 2D). Hoechst 33342 staining was more diffuse throughout the cells but also showed lower nuclear staining, which was most likely to be a result of nuclear condensation (Fig. 2E). Propidium iodide could not be used with these cells because the doxorubicin was red (data not shown). Rod-shaped cells were YO-PRO-1 positive for apoptosis following doxorubicin induction (Fig. 2F). We therefore concluded that the isolation and culture procedures were not pro-apoptotic and that the decrease in the ratio of rod-shaped cell number to round-shaped cell number was a result of cellular necrosis.

Contractility measurements

Figure 3A shows representative recordings of sarcomere length shortening and calcium transient recorded in the

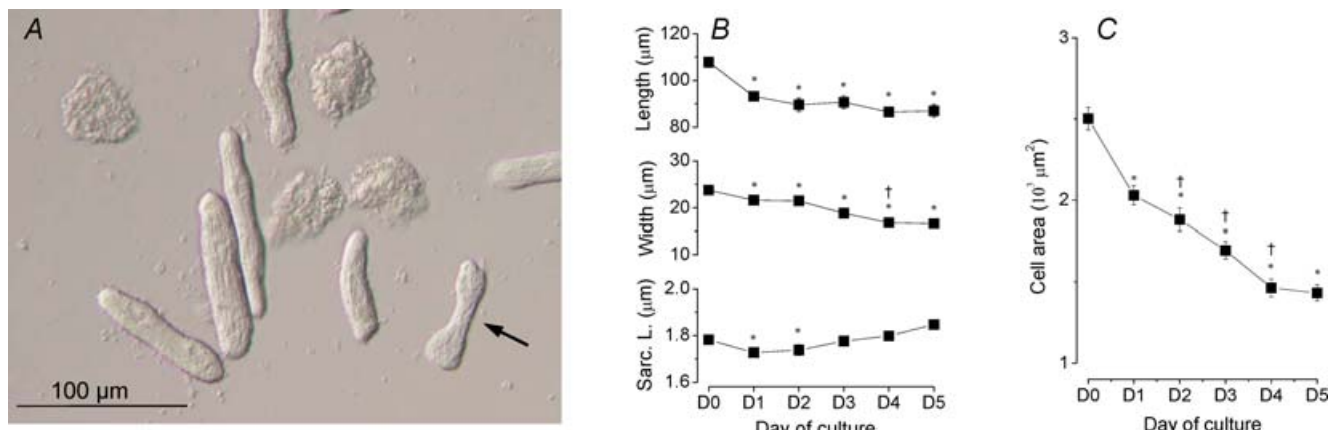


Figure 1. Morphometric changes of cultured adult rat ventricular cardiomyocytes

A, phase contrast image of 5-day-old cardiomyocyte culture. The majority of cells preserved rod shape and striation. B and C, morphometric data of ARVM in cultures. Sarc. L., sarcomere length. Values were obtained in 72–124 cells from 6 animals/cultures. * $P < 0.05$ versus data obtained in freshly isolated cells (Student's paired *t* test). † $P < 0.05$ versus data shown at immediate left (paired *t* test)

same ARVM at various frequencies on the day of cell isolation (D0). Figure 3B and C shows that diastolic sarcomere length and systolic shortening of ARVM decreased at higher stimulation rates on D0, D1 and D2. The negative force–frequency relationship (referred to as negative Bowditch effect) is characteristic of rat myocardium in the frequency range studied (Endoh, 2004). Our data show that this feature of myocytes was maintained up to the second culture day; however, diastolic sarcomere length was found to be shorter at each stimulating frequency on D1 and D2 compared with D0. There was no significant decrease in the systolic shortening amplitude during the same period at each frequency studied. The systolic shortening was

significantly smaller after D2 at lower pacing rates and the frequency dependence was no longer present. Parallel to this, the frequency dependence of diastolic sarcomere length was less steep. The fractional sarcomere length shortening was higher than 7% (at 0.1 Hz pacing rate) in every cell on the day of isolation. However, after D2 all cells had fractional sarcomere length shortening less than 2%. Diastolic fluorescence intensity (Fig. 3D) was not altered by pacing rate or length of culture in ARVM measured with fluo-5F ($P >> 0.05$ with single-factor ANOVA). Systolic fluorescence intensity showed no frequency dependence in freshly isolated cells or during the period of culturing. However, we observed a significant decrease in systolic fluorescence intensity along the culture time (Fig. 3E).

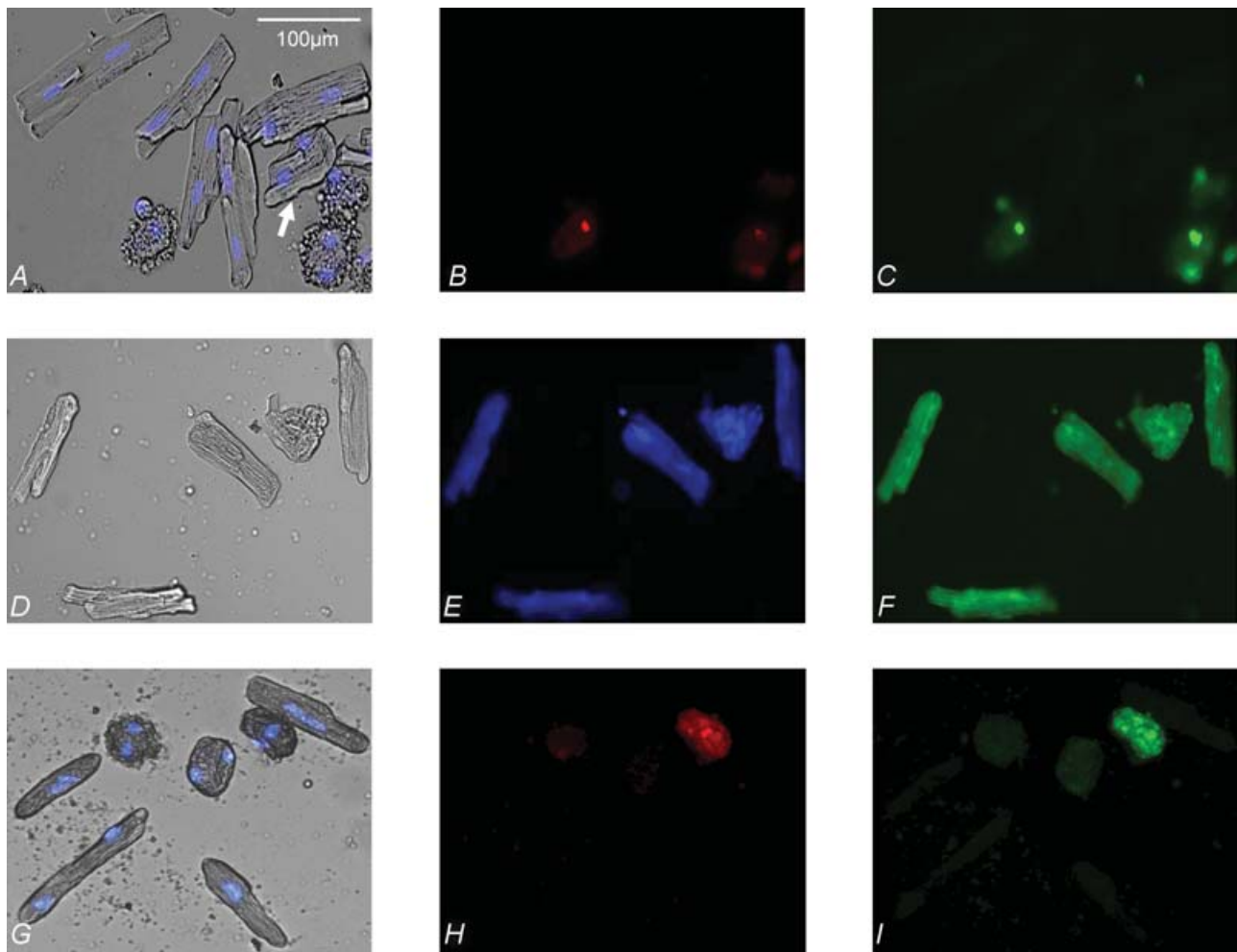


Figure 2. Viability assay of freshly isolated and cultured ARVM

A–C, freshly isolated myocytes. A, Hoechst 33342 staining, with which nuclear chromatin fluoresces blue. Arrow points to a cell with partial deterioration. B, propidium iodide staining, with which dead cells fluoresce red. C, YO-PRO 1 staining, with which dead and apoptotic cells fluoresce green. D–F, 5 μ M doxorubicin-treated myocytes. D, bright field image of cultured myocytes after 14 h doxorubicin induction. E, Hoechst 33342 staining of induced cells. Chromatin condensation and nuclear fragmentation is visible. F, YO-PRO-1 staining for apoptosis. G–I, day 5 cultures, with Hoechst 33342 (G), propidium iodide (H) or YO-PRO-1 staining (I). Only rounded cells are fluorescently detected.

Staining of T-tubules

To study whether contractile dysfunction, observed during prolonged culture, was associated with T-tubule degradation, we determined the T-tubule area relative to cell area (RTTA) in ARVM on each culture day. Figure 4A–C shows representative images recorded on D0, D3 and D5, respectively. Freshly isolated (D0) cells displayed well-developed and well-organized T-tubule structure visualized with di-8-ANEPPS. The T-tubule structure became fragmented during the first two culture days, and RTTA showed a significant decrease. Owing to the relatively high variability of RTTA in cultured cells, we found it more demonstrative to construct a distribution diagram of RTTA. As shown in Fig. 4F, RTTA distribution shifted towards lower RTTA values during prolonged culture. Following D3, we found no cells with larger RTTA than 20%.

In order to validate our method of RTTA assessment we used formamide treatment to acutely detubulate the cells and determined RTTA in two groups of detubulated cells. In the first group of cells, we stained freshly isolated cells after detubulation (Fig. 4D). We found that, under these circumstances, RTTA was much less than in the D0 control group (Fig. 4G). When detubulation followed di-8-ANEPPS staining, RTTA did not decrease (data not shown); however, T-tubule structure was fragmented (Fig. 4E). These tests indicate that di-8-ANEPPS can stain T-tubules only when they are connected to sarcolemma. Therefore, decreased RTTA during prolonged culture might result from detachment of T-tubules from sarcolemma and does not necessarily indicate a complete degradation of the T-tubule system.

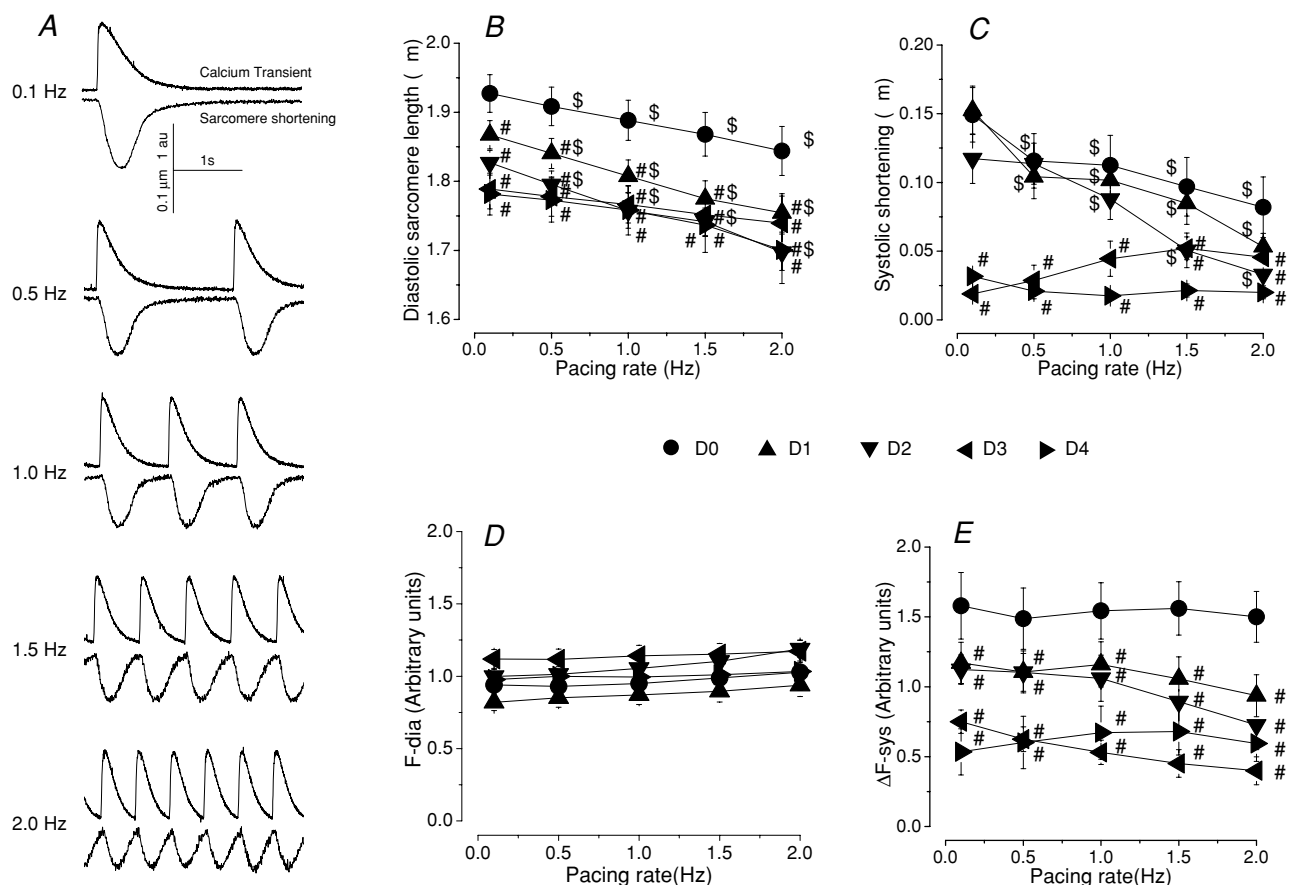


Figure 3. Contractile properties of ARVM

A, simultaneously recorded calcium transient and cell shortening traces from freshly isolated ARVM recorded at different pacing rates. Both diastolic (B) and systolic sarcomere length (C) display a negative frequency relationship in freshly isolated ARVM. Systolic sarcomere length shortening decreased significantly after D2, and the frequency dependence disappeared. Diastolic calcium signal (F-dia; D) showed no frequency dependence over culture time. The systolic value of the calcium transient (F-sys) did not show frequency dependence (E), but decreased significantly during culture. $n = 7–12$ for each group. ${}^{\$}P < 0.05$ versus 0.1 Hz data on the same culture day (Student's paired t test). ${}^{\#}P < 0.05$ versus data obtained in freshly isolated cells at the same pacing rate (Student's unpaired t test).

Electrophysiology

As expected from morphometric data, membrane capacitance (C_m) decreased during culture (Fig. 5A). In the D3 myocytes, C_m was lower by 32% than that of the freshly isolated cells (105 ± 11 and 156 ± 8 pF, respectively), but no further decrease was observed during D4 and D5. Interestingly, C_m in detubulated cells was similar to that in D3, D4 and D5 cells.

The action potential duration (APD) of freshly isolated ARVM lengthened in each cell when the pacing rate was increased (Fig. 5B). However, cell-to-cell variations of APD at any stimulation rate examined were larger than frequency-induced lengthening within the same myocyte. For example, the average lengthening of APD₉₀ (Action Potential Duration measured at 90% repolarization) when pacing rate was increased from 0.1 to 1.0 Hz was 3.3 ± 2.1 ms. At the same time, the standard errors of

APD₉₀ measured at 0.1 and 1.0 Hz pacing rate were 3.5 and 2.9 ms, respectively. Therefore, frequency-induced differences were found to be statistically not significant with both ANOVA and correlation analysis.

The average resting membrane potential was -77.3 ± 2.5 mV on the day of cell isolation. Our cells were found to be significantly depolarized following the first day of culture (59.6 ± 6.1 mV $P < 0.01$), and we observed only a slow response in these cells. However, application of a relatively small (100–200 pA) hyperpolarizing current restored the membrane potential to the normal range and cells were then able to generate regular action potentials (Fig. 5C). The membrane potential decreased progressively during the five culture days examined, reaching -24.2 ± 5.97 mV on day 5 (Fig. 5F). To investigate the electrophysiological background of the depolarization, we tested I_{K1} in our cells using the

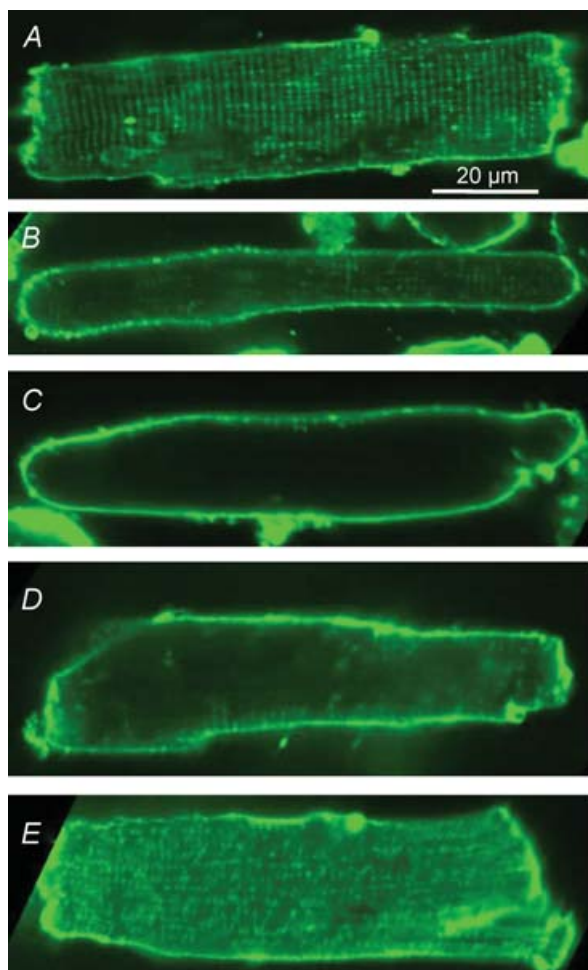
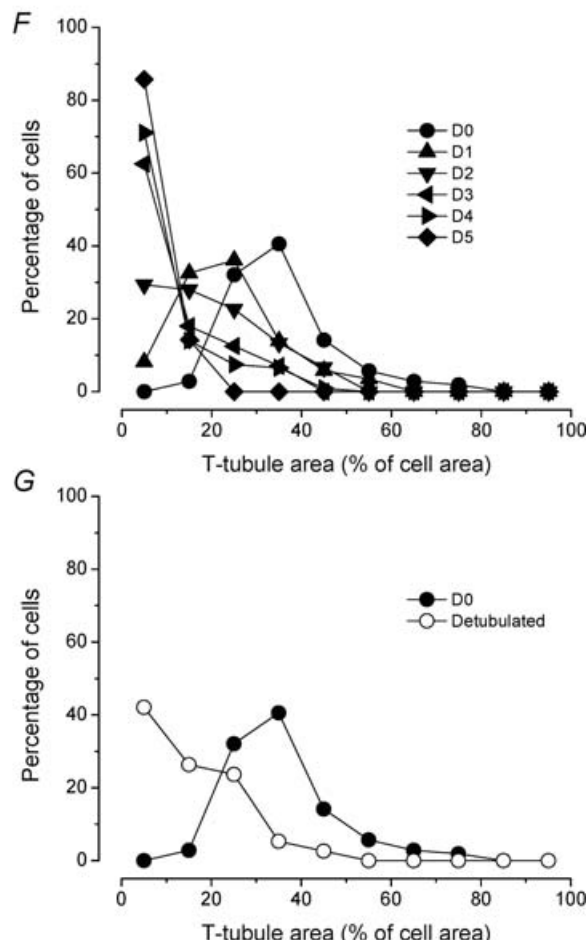


Figure 4. Decreased di-8-ANEPPS staining of T-tubules in cultured and detubulated ARVM

Representative confocal scanning micrographs of ARVM following isolation (A) and cultured for 3 (B) and 5 days (C). Acutely detubulated cells showed decreased di-8-ANEPPS staining (D). When acute detubulation was performed after di-8-ANEPPS staining of the T-tubules, relative T-tubule area (RTTA) was not decreased; however, T-tubule fragmentation was observed (E). Also shown is a frequency diagram for RTTA on different days of culture (F) and for detubulated versus freshly isolated ARVM (G). $n = 107$ –128 cells for each group from 7 animals.



barium-sensitive component of transmembrane current during a -120 mV test pulse from a holding potential of -70 mV (Fig. 5D). Between D0 and D5 the barium-sensitive current showed a continuous decrease of 35% (Fig. 5E), whereas the current amplitude was significantly lower in detubulated cells (D0). The relationship between resting membrane potential and I_{K1} density is presented in Fig. 5F. Our data show that decreased I_{K1} density is associated with lower resting membrane potential. These results indicate that the decreased I_{K1} density is an important determinant of the progressive depolarization observed in ARVM during culture. Figure 6A and B shows representative $I_{Ca,L}$ families from freshly isolated cells and peak current density–voltage relationships for D0,

D5 and detubulated cells. The peak current amplitude of $I_{Ca,L}$ (measured at $+10$ mV) decreased during culture and following detubulation (Fig. 6C) but we found no difference in the kinetic properties of $I_{Ca,L}$ (Table 1).

Discussion

Several lines of evidence suggest that cardiomyocytes undergo profound transformation during long-term culture. First, under all culture conditions, 50–70% of rat cardiomyocytes are lost during the first week of culture (Schwarzfeld & Jacobson, 1981; Haddad *et al.* 1988; Spahr *et al.* 1989; Dubus *et al.* 1990). Second, among other morphological and functional changes detected,

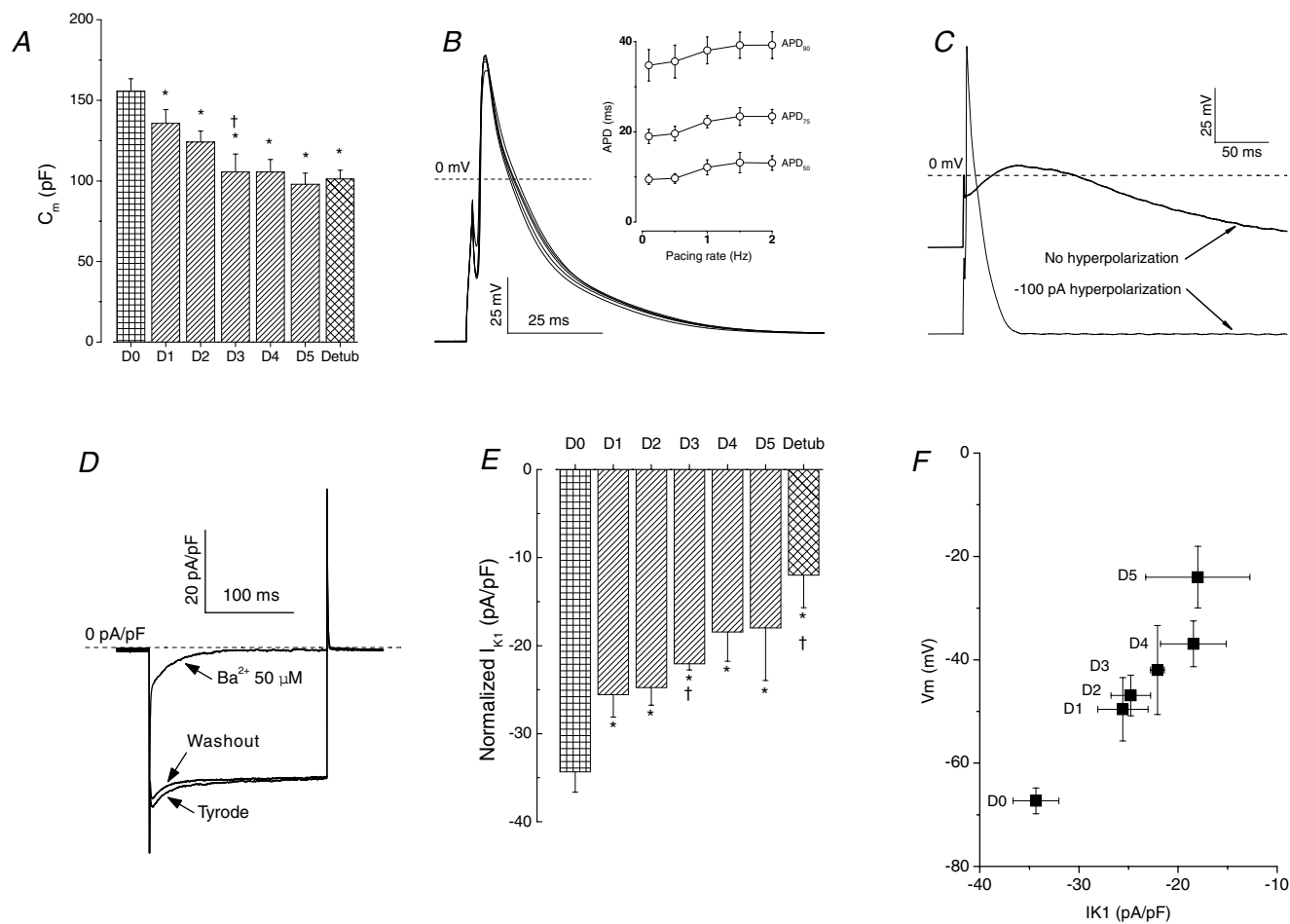


Figure 5. Changes in electrophysiological parameters of ARVM during culture

A, average cell capacitances for freshly isolated, cultured and detubulated ARVM. *B*, representative action potentials in freshly isolated ARVM recorded at different pacing rates between 0.1 and 2 Hz. Inset shows rate-dependent lengthening of action potentials ($n = 5$). *C*, representative action potentials of ARVM recorded on D3. A slow action potential was seen under current clamp conditions. Application of 100 pA hyperpolarizing current restored a normal action potential in cultured ARVM. *D*, representative recording of barium-sensitive current elicited with a step to -130 mV from a holding potential of -70 mV. *E*, I_{K1} decreased gradually during culture. Detubulation decreased I_{K1} by 65%. $^*P < 0.05$ versus data obtained in freshly isolated cells (Student's paired *t* test). $\dagger P < 0.05$ versus data shown immediately to the left (Student's paired *t* test) *F*, plot of resting membrane potential of cultured ARVM against their respective values of I_{K1} on different culture days.

Table 1. Kinetic properties of $I_{Ca,L}$ in freshly isolated, cultured and detubulated ARVM

	D0	D1	D2	D3	D4	D5	Detubulated
SSI $V_{0.5}$ (mV)	13.21 ± 1.43	12.86 ± 0.38	10.19 ± 2.03	11.32 ± 1.80	8.07 ± 1.84	12.64 ± 2.09	11.31 ± 2.09
SSI Slope	5.52 ± 0.46	5.16 ± 0.09	4.75 ± 0.15	4.62 ± 0.19	4.95 ± 0.10	4.32 ± 0.13	5.05 ± 0.09
G_{max} $V_{0.5}$ (mV)	1.06 ± 1.62	1.59 ± 0.47	3.85 ± 2.49	3.74 ± 2.63	6.46 ± 2.70	6.28 ± 3.09	3.03 ± 2.77
G_{max} Slope	5.59 ± 0.18	5.37 ± 0.11	6.17 ± 0.53	5.16 ± 0.40	6.50 ± 0.69	6.49 ± 0.57	5.57 ± 0.25

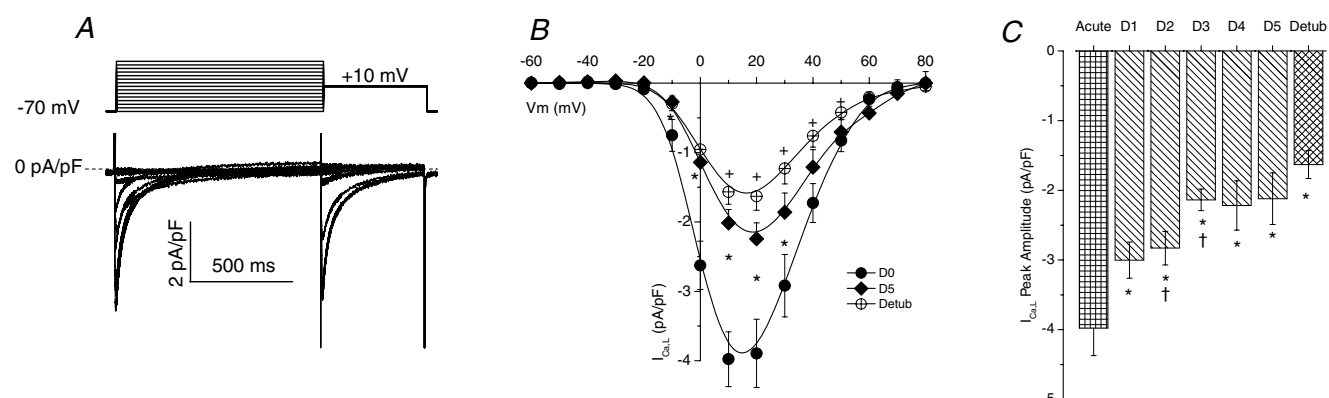
No significant differences were found with ANOVA. SSI, Steady-state inactivation; G_{max} , Maximum conductance.

internalization of intercalated disks (Jacobson & Piper, 1986), decreased transverse tubule density (Mitchelson *et al.* 1998; Louch *et al.* 2004; Leach *et al.* 2005; Gorelik *et al.* 2006), altered calcium signalling mechanisms (Poindexter *et al.* 2001; Louch *et al.* 2004) and reduced contractility, as well as decreased resting membrane potential and L-type calcium current density (Ellingsen *et al.* 1993; Leach *et al.* 2005), were reported in adult rat cardiomyocyte culture. Third, a number of attempts made by several groups to design culture conditions to maintain the cardiomyocyte phenotype and function in long-term primary culture (Ellingsen *et al.* 1993; Berger *et al.* 1994; Davidoff *et al.* 1997; Horackova *et al.* 1997; Polonchuk *et al.* 2000; Akuzawa-Tateyama *et al.* 2006) show that cultured cardiomyocytes do not maintain a steady state and cannot replace acutely isolated cardiomyocytes as an experimental model.

While early studies focused on either morphological or certain functional changes observed in long-term cell culture, the present study is the first to provide detailed information to correlate morphological changes with functional alterations under the same culture conditions. Our results indicate that changes in cell morphology, contractility and membrane electrophysiology start on the first culture day (D1). We found that average cell size

(length, width and area) decreases continuously during culture, or another possibility is that the ratio of small cells increases in the surviving population during culture.

To examine the mechanism of cell death in culture, we assayed apoptotic and necrotic activity on each culture day. We concluded that as long as ARVM are able to maintain rod-shaped morphology or only partial deterioration is observed, they display neither apoptotic nor necrotic activity. Therefore, the mechanism responsible for rounding up ARVM is not initiated by apoptotic or necrotic activity. This conclusion is supported by earlier data of Kuramochi *et al.* (2004), who used Trypan Blue staining to measure cell viability in culture. On the photomicrographs they presented, one can clearly see that not only rod-shaped cells, but a considerable fraction of the round-shaped cells are Trypan Blue negative. We also assayed our cells with Trypan Blue (data not shown) and found that rod-shaped ARVM are always Trypan Blue negative, and only a fraction of rounded cells are positive. Considering that major sarcomere length shortening was not observed (Fig. 1B) and that diastolic calcium was not increased (Fig. 3D), we have to conclude that the normal diastolic calcium level is maintained in rod-shaped cells. At the same time, we detected progressive depolarization of resting membrane

**Figure 6.** L-type calcium current in freshly isolated, cultured and detubulated ARVM

A, representative current family and pulse protocol for freshly isolated ARVM. *B*, current density–voltage relationship for freshly dissociated ARVM ($n = 7$), detubulated ARVM ($n = 7$) and ARVM cultured for 5 days ($n = 5$ –9 for each culture day). *C*, peak $I_{Ca,L}$ densities evoked by depolarization to +10 mV from a holding potential of -70 mV for freshly isolated, cultured and detubulated ARVM. Calcium current density decreased gradually during culture. * $P < 0.05$ versus data obtained in freshly isolated cells (Student's paired *t* test). † $P < 0.05$ versus data shown immediately to the left (Student's paired *t* test).

potential, reduced $I_{Ca,L}$ and I_{K1} densities, reduced calcium transient amplitudes and fractional shortening in rod-shaped cells. Taking these observations together, we conclude that cellular functions deteriorate in cultured ARVM (i.e. the cell can maintain normal diastolic calcium concentrations but not physiological resting membrane potential) and that morphological parameters alone (such as cell length or diastolic sarcomere length) cannot present reliable diagnostic information on the general condition of cultured myocytes.

Our data show that the most profound changes in functional parameters take place around the third culture day. Di-8-ANEPPS shows no visible staining of T-tubule structure in cells after D3 (Fig. 4C). The RTTA was less than 10% in most cultured cells on D3 (Fig. 4F), and this value can be attributed mainly to the sarcolemma. The third culture day was also a critical transition point for the majority of other functional parameters. The negative Bowditch effect was diminished after D3 (Fig. 3C), and $I_{Ca,L}$ density, systolic calcium transient, systolic shortening and C_m also reached a minimal level. Interestingly, minimal values for C_m and $I_{Ca,L}$ were in good agreement with those measured in detubulated cells (Fig. 5A). This correlation serves as further (indirect) support that detubulation occurs in ARVM during long-term culture.

While our morphological and functional data mostly show good correlations, we can point to apparent controversies as well. Average sarcomere length was longer in our contraction measurements (Fig. 3B) than that shown in morphometric data (Fig. 1B). This difference, as well as the different extent of shortening during culture, might arise from the different ionic milieu used during these measurements. Morphometric data were measured in cell culture medium, while contractility was recorded in Tyrode solution (among other differences, the calcium concentration is 1.26 mM in culture medium and 1.0 mM in Tyrode solution).

Reduction in T-tubule density of cardiomyocytes during culture has been reported but, apart from a recent paper from Louch *et al.* (2004), no attempt has been made to quantify the observations. Louch and colleagues reported 86% reduction of T-tubule signal at 72 h culture in pig cardiomyocytes using di-8-ANEPPS staining. We observed a similar reduction in RTTA in cultured ARVM with the same method (Fig. 4F). However, our observations on detubulated cells indicate that decreased di-8-ANEPPS staining might also result from detachment of T-tubules from the sarcolemma even with partly preserved T-tubule structure inside the cell (Fig. 4D and E). The di-8-ANEPPS was applied in the extracellular solution; therefore, membrane structures not connected directly to the sarcolemma (such as sarcoplasmic reticulum or T-tubules detached from the surface membrane) are 'invisible' with this method. Thus, we cannot exclude

the possibility that, despite the reduced (or lack of) di-8-ANEPPS staining, the T-tubule system could be preserved to some extent in cultured cardiomyocytes. It is unclear, however, what the functional consequence of T-tubule detachment from the surface membrane would be.

We found good correlation between the progressive decrease in I_{K1} and resting membrane potential in cultured ARVM (Fig. 5F). The loss of ion channels may be related to the reduction in T-tubule density. Several publications support the suggestion that the $K_{ir2.1}$ channel, which underlies the inward rectifier current I_{K1} , is located predominantly in the T-tubules (Clark *et al.* 2001; Brette & Orchard, 2003), although one study showed that detubulation did not reduce I_{K1} normalized to cell capacitance (Komukai *et al.* 2002). In our experiments, normalized I_{K1} was significantly decreased following detubulation, and we observed a progressive decrease in I_{K1} current density parallel with detubulation in culture. The difference might be explained by the different degree of detubulation in various studies. The reduction in cell capacitance was 26.2% in Kawai's study and 35.0% in our study. Thus, our observations support the suggestion that I_{K1} channels are localized predominantly in the T-tubules, which leads us to the conclusion that loss of T-tubules is an important factor in depolarization of cultured ARVM. The same differences in the degree of detubulation can be responsible for the discrepancy of the action potential contour of detubulated cells observed in our study and that of Brette *et al.* (2006). Detubulation resulted in shortening of the action potential, and no depolarization was observed in the report of Brette *et al.* (2006). We found significant depolarization in our freshly isolated myocytes following detubulation to a level where no action potential, but slow response, can be evoked. The reduction in cell capacitance following acute detubulation was 35.0% in our cells *versus* 28.5% in Brette's study. If I_{K1} is located predominantly in T-tubules, a large difference in current density can result from a relatively small difference in T-tubule area.

In normal heart, contraction is initiated by an action potential, and the activation signal is synchronized by the T-tubule system. Since our ARVM lack a normal action potential in long-term culture but still contract under field stimulation, we might deduce that L-type calcium current and the Na^+-Ca^{2+} exchanger will deliver calcium ions during a slow action potential to initiate contraction. The wide plasticity of both the L-type calcium channel and the Na^+-Ca^{2+} exchanger mechanism, known from earlier studies (Leblanc & Hume, 1990; Litwin *et al.* 1996; Vites & Wasserstrom, 1996; Wasserstrom & Vites, 1996; Reuter *et al.* 2003, 2005), makes this adaptation plausible.

Detubulation and excitation–contraction coupling has already been extensively investigated in cardiac myocytes by Dr C. H. Orchard and colleagues (Kawai *et al.* 1999;

Brette & Orchard, 2003; Leach *et al.* 2005; Brette *et al.* 2006; Pasek *et al.* 2007). Their observations provide strong evidence that the T-tubules are a key site for the regulation of action potential contour and calcium entry into the cytoplasm. Our data are in good agreement with their observations regarding the ~50% decrease in $I_{Ca,L}$ density and ~30% decrease in cell capacitance following acute detubulation in freshly isolated cardiac myocytes (Brette *et al.* 2006). Since calcium entry at the T-tubules is larger than that at surface sarcolemma (Brette *et al.* 2006; Pasek *et al.* 2007), this ~30% decrease in cell capacitance can be responsible for the loss of the majority of calcium entry required for contraction. Furthermore, Brette *et al.* (2006) suggested that calcium entry at the cell surface provides Ca^{2+} for the sarcoplasmic reticulum, but the T-tubule system allows synchronous calcium release across the cell. This proposal was also supported by the observations of Louch *et al.* (2004). Thus, we conclude that detubulation, which results in only ~50% reduction of $I_{Ca,L}$, can lead to complete loss of contractility (Fig. 3).

In summary, the present paper provides a quantitative description of the progressive morphological and functional changes observed in cultured ARVM. Our data indicate that the observed morphological or functional alterations cannot be attributed to apoptosis or necrosis. The progressive nature of the observed changes and the correlation among the parameters studied makes it very likely that these alterations are induced by complex adaptation to the new environment in the culture. These changes put limits on using cultured adult cardiac myocytes for functional studies and need to be considered in the interpretation of experimental data acquired from cultured ARVM.

References

Akuzawa-Tateyama M, Tateyama M & Ochi R (2006). Sustained b-adrenergic stimulation increased L-type Ca^{2+} channel expression in cultured quiescent ventricular myocytes. *J Physiol Sci* **56**, 165–172.

Arruda LH, Cestari IA, Leirner AA & Cestari IN (2007). Adenoviral expression of calmodulin antisense reduces hypertrophy in cultured cardiomyocytes. *Artif Organs* **31**, 274–277.

Berger HJ, Prasad SK, Davidoff AJ, Pimental D, Ellingsen O, Marsh JD, Smith TW & Kelly RA (1994). Continual electric field stimulation preserves contractile function of adult ventricular myocytes in primary culture. *Am J Physiol Heart Circ Physiol* **266**, H341–H349.

Bölk B, Münch G, Mackenstein P, Hellmich M, Hirsch I, Reuter H, Hattebuh N, Weig HJ, Ungerer M, Brixius K & Swinger RH (2004). Na^{+}/Ca^{2+} exchanger overexpression impairs frequency- and ouabain-dependent cell shortening in adult rat cardiomyocytes. *Am J Physiol Heart Circ Physiol* **287**, H1435–H1445.

Brette F & Orchard C (2003). T-tubule function in mammalian cardiac myocytes. *Circ Res* **92**, 1182–1192.

Brette F, Salle L & Orchard CH (2006). Quantification of calcium entry at the T-tubules and surface membrane in rat ventricular myocytes. *Biophys J* **90**, 381–389.

Chilton L, Giles W & Smith GL (2007). Evidence of intercellular coupling between co-cultured adult rabbit ventricular myocytes and myofibroblasts. *J Physiol* **583**, 225–236.

Clark RB, Tremblay A, Melnyk P, Allen BG, Giles WR & Fiset C (2001). T-tubule localization of the inward-rectifier K^{+} channel in mouse ventricular myocytes: a role in K^{+} accumulation. *J Physiol* **537**, 979–992.

Cuello F, Bardswell SC, Haworth RS, Yin X, Lutz S, Wieland T, Mayr M, Kentish JC & Avkiran M (2007a). Protein kinase D selectively targets cardiac troponin I and regulates myofilament Ca^{2+} sensitivity in ventricular myocytes. *Circ Res* **100**, 864–873.

Cuello F, Snabaitis AK, Cohen MS, Taunton J & Avkiran M (2007b). Evidence for direct regulation of myocardial Na^{+}/H^{+} exchanger isoform 1 phosphorylation and activity by 90-kDa ribosomal S6 kinase (RSK): effects of the novel and specific RSK inhibitor fmk on responses to α_1 -adrenergic stimulation. *Mol Pharmacol* **71**, 799–806.

Davidoff AJ, Maki TM, Ellingsen O & Marsh JD (1997). Expression of calcium channels in adult cardiac myocytes is regulated by calcium. *J Mol Cell Cardiol* **29**, 1791–1803.

Dubus I, Samuel JL, Marotte F, Delcayre C & Rappaport L (1990). β Adrenergic agonists stimulate the synthesis of noncontractile but not contractile proteins in cultured myocytes isolated from adult rat heart. *Circ Res* **66**, 867–874.

Eder P, Probst D, Rosker C, Poteser M, Wolinski H, Kohlwein SD, Romanin C & Groschner K (2007). Phospholipase C-dependent control of cardiac calcium homeostasis involves a TRPC3-NCX1 signaling complex. *Cardiovasc Res* **73**, 111–119.

Ellingsen O, Davidoff AJ, Prasad SK, Berger HJ, Springhorn JP, Marsh JD, Kelly RA & Smith TW (1993). Adult rat ventricular myocytes cultured in defined medium: phenotype and electromechanical function. *Am J Physiol Heart Circ Physiol* **265**, H747–H754.

Endoh M (2004). Force-frequency relationship in intact mammalian ventricular myocardium: physiological and pathophysiological relevance. *Eur J Pharmacol* **500**, 73–86.

Gorelik J, Yang LQ, Zhang Y, Lab M, Korchev Y & Harding SE (2006). A novel Z-groove index characterizing myocardial surface structure. *Cardiovasc Res* **72**, 422–429.

Haddad J, Decker ML, Hsieh LC, Lesch M, Samarel AM & Decker RS (1988). Attachment and maintenance of adult rabbit cardiac myocytes in primary cell culture. *Am J Physiol Cell Physiol* **255**, C19–C27.

Heidkamp MC, Iyengar R, Szotek EL, Cribbs LL & Samarel AM (2007). Protein kinase-C ϵ -dependent MARCKS phosphorylation in neonatal and adult rat ventricular myocytes. *J Mol Cell Cardiol* **42**, 422–431.

Herron TJ, Vandenboom R, Fomicheva E, Mundada L, Edwards T & Metzger JM (2007). Calcium-independent negative inotropy by β -myosin heavy chain gene transfer in cardiac myocytes. *Circ Res* **100**, 1182–1190.

Horackova M & Byczko Z (1997). Differences in the structural characteristics of adult guinea pig and rat cardiomyocytes during their adaptation and maintenance in long-term cultures: confocal microscopy study. *Exp Cell Res* **237**, 158–175.

Horackova M, Byczko Z & Maillet-Frotten L (1997). Immunohistochemical analysis of the adaptation of adult guinea-pig cardiomyocytes in long-term cultures and in cocultures with cardiac neurons: a novel model for studies of myocardial function. *Mol Cell Biochem* **172**, 227–238.

Horackova M, Croll RP, Hopkins DA, Losier AM & Armour JA (1996). Morphological and immunohistochemical properties of primary long-term cultures of adult guinea-pig ventricular cardiomyocytes with peripheral cardiac neurons. *Tissue Cell* **4**, 411–425.

Huang Y, Wright CD, Merkwan CL, Baye NL, Liang Q, Simpson PC & O'Connell TD (2007). An α_{1A} -adrenergic-extracellular signal-regulated kinase survival signaling pathway in cardiac myocytes. *Circulation* **115**, 763–772.

Jacobson SL & Piper HM (1986). Cell cultures of adult cardiomyocytes as models of the myocardium. *J Mol Cell Cardiol* **18**, 661–678.

Kawai M, Hussain M & Orchard CH (1999). Excitation-contraction coupling in rat ventricular myocytes after formamide-induced detubulation. *Am J Physiol Heart Circ Physiol* **277**, 603–609.

Komukai K, Brette F, Yamanishi TT & Orchard CH (2002). K⁺ current distribution in rat sub-epicardial ventricular myocytes. *Pflugers Arch* **444**, 532–538.

Kumar D, Kirshenbaum L, Li T, Danelisen I & Singal P (1999). Apoptosis in isolated adult cardiomyocytes exposed to adriamycin. *Ann NY Acad Sci* **874**, 156–168.

Kuramochi Y, Lim CC, Guo X, Colucci WS, Liao R & Sawyer DB (2004). Myocyte contractile activity modulates norepinephrine cytotoxicity and survival effects of neuregulin-1. *Am J Physiol Cell Physiol* **286**, C222–C229.

Leach RN, Desai JC & Orchard CH (2005). Effect of cytoskeleton disruptors on L-type Ca channel distribution in rat ventricular myocytes. *Cell Calcium* **38**, 515–526.

Leblanc N & Hume JR (1990). Sodium current-induced release of calcium from cardiac sarcoplasmic reticulum. *Science* **248**, 372–376.

Litwin S, Kohomoto O, Levi AJ, Spitzer KW & Bridge JH (1996). Evidence that reverse Na⁺/Ca²⁺ exchange can trigger SR calcium release. *Ann NY Acad Sci* **779**, 451–463.

Lopez-Lopez JR (1995). Local calcium transients triggered by single L-type calcium channel currents in cardiac cells. *Science* **268**, 1042–1045.

Lou H, Kaur K, Sharma AK & Singal PK (2006). Adriamycin-induced oxidative stress, activation of MAP kinases and apoptosis in isolated cardiomyocytes. *Pathophysiology* **13**, 103–109.

Louch WE, Bito V, Heinzel FR, Macianskiene R, Vanhaecke J, Flameng W, Mubagwa K & Sipido KR (2004). Reduced synchrony of Ca²⁺ release with loss of T-tubules – a comparison to Ca²⁺ release in human failing cardiomyocytes. *Cardiovasc Res* **62**, 63–73.

Mitchelson JS, Hancox JC & Levi AJ (1998). Cultured adult cardiac myocytes: future applications, culture methods, morphological and electrophysiological properties. *Cardiovasc Res* **39**, 280–300.

Oestreich EA, Wang H, Malik S, Kaproth-Joslin KA, Blaxall BC, Kelley GG, Dirksen RT & Smrcka AV (2007). Epac-mediated activation of phospholipase C ϵ plays a critical role in β -adrenergic receptor-dependent enhancement of Ca²⁺ mobilization in cardiac myocytes. *J Biol Chem* **282**, 5488–5495.

Pasek M, Simurda J, Christe G & Orchard CH (2007). Modelling the cardiac transverse-axial tubular system. *Prog Biophys Mol Biol*. In press.

Poindexter BJ, Smith JR, Buja LM & Bick RJ (2001). Calcium signaling mechanisms in dedifferentiated cardiac myocytes: comparison with neonatal and adult cardiomyocytes. *Cell Calcium* **30**, 373–382.

Polonchuk L, Elbel J, Eckert L, Blum J, Wintermantel E & Eppenberger HM (2000). Titanium dioxide ceramics control the differentiated phenotype of cardiac muscle cells in culture. *Biomaterials* **21**, 539–545.

Reuter H, Henderson SA, Han T, Mottino GA, Frank JS, Ross RS, Goldhaber JI & Philipson KD (2003). Cardiac excitation-contraction coupling in the absence of Na⁺–Ca²⁺ exchange. *Cell Calcium* **34**, 19–26.

Reuter H, Pott C, Goldhaber JI, Henderson SA, Philipson KD & Schwinger RH (2005). Na⁺/Ca²⁺ exchange in the regulation of cardiac excitation-contraction coupling. *Cardiovasc Res* **67**, 198–207.

Schiess MC, Poindexter BJ, Brown BS & Bick RJ (2005). The effects of CGRP on calcium transients of dedifferentiating cultured adult rat cardiomyocytes compared to non-cultured adult cardiomyocytes: possible protective and deleterious results in cardiac function. *Peptides* **26**, 525–530.

Schwarzfeld TA & Jacobson SL (1981). Isolation and development in cell culture of myocardial cells of the adult rat. *J Mol Cell Cardiol* **13**, 563–575.

Spahr R, Jacobson SL, Siegmund B, Schwartz P & Piper HM (1989). Substrate oxidation by adult cardiomyocytes in long-term primary culture. *J Mol Cell Cardiol* **21**, 175–185.

Tastan H, Abdallah Y, Euler G, Piper HM & Schlüter KD (2007). Contractile performance of adult ventricular rat cardiomyocytes is not directly jeopardized by NO/cGMP-dependent induction of pro-apoptotic pathways. *J Mol Cell Cardiol* **42**, 411–421.

Vila-Petroff M, Salas MA, Said M, Valverde CA, Sapia L, Portiansky E, Hajjar RJ, Kranias EG, Mundina-Weilenmann C & Mattiazzi A (2007). CaMKII inhibition protects against necrosis and apoptosis in irreversible ischemia-reperfusion injury. *Cardiovasc Res* **73**, 689–698.

Vites AM & Wasserstrom JA (1996). Fast sodium influx provides an initial step to trigger contractions in cat ventricle. *Am J Physiol Heart Circ Physiol* **40**, H674–H686.

Volz A, Piper HM, Siegmund B & Schwartz P (1991). Longevity of adult ventricular rat heart muscle cells in serum-free primary culture. *J Mol Cell Cardiol* **23**, 161–173.

Warriner S, Ramamurthy G, Eckert RL, Nikolaev VO, Lohse MJ & Harvey RD (2007). cAMP microdomains and L-type Ca²⁺ channel regulation in guinea-pig ventricular myocytes. *J Physiol* **580**, 765–776.

Wasserstrom JA & Vites AM (1996). The role of $\text{Na}^+/\text{Ca}^{2+}$ exchange in activation of excitation–contraction coupling in rat ventricular myocytes. *J Physiol* **493**, 529–542.

Weisser-Thomas J, Dieterich E, Janssen PM, Schmidt-Schewda S, Maier LS, Sumbilla C & Pieske B (2005). Method-related effects of adenovirus-mediated LacZ and SERCA1 gene transfer on contractile behavior of cultured failing human cardiomyocytes. *J Pharmacol Toxicol Methods* **51**, 91–103.

Yang D, Zhu WZ, Xiao B, Brochet DX, Chen SR, Lakatta EG, Xiao RP & Cheng H (2007). Ca^{2+} /calmodulin kinase II-dependent phosphorylation of ryanodine receptors suppresses Ca^{2+} sparks and Ca^{2+} waves in cardiac myocytes. *Circ Res* **100**, 399–407.

Zhu W, Woo AY, Yang D, Cheng H, Crow MT & Xiao RP (2007). Activation of CaMKII_C is a common intermediate of diverse death stimuli-induced heart muscle cell apoptosis. *J Biol Chem* **282**, 10833–10839.

Acknowledgements

We thank Sidney W. Whiteheart (University of Kentucky, College of Medicine, Department of Molecular and Cellular Biochemistry, NIH P20 RR-03-014) for the use of microscope core facility and technical assistance. This work was supported by AHA National Scientist Development Grant (O335250N), NIH-K25 (HL068704) and NIH-RO1 (HL68733).